Eur Biophys J (2001) 30: 207–220
DOI 10.1007/s002490000127

ARTICLE

Kouji Kinoshita · Shu Jie Li · Masahito Yamazaki

The mechanism of the stabilization of the hexagonal II (H_{II}) phase in phosphatidylethanolamine membranes in the presence of low concentrations of dimethyl sulfoxide

Received: 30 August 2000 / Revised version: 13 November 2000 / Accepted: 17 November 2000 / Published online: 6 March 2001

Abstract Dimethyl sulfoxide (DMSO), a water-miscible organic solvent, has been used as a cryoprotectant for cells. It is known that DMSO stabilizes the H_{II} phase of phosphatidylethanolamine (PE) membranes rather than the L_α phase, while most other water-miscible organic solvents such as acetone and ethanol destabilize the H_{II} phase. To elucidate the mechanism for this stabilizing effect of DMSO on the H_{II} phase, we have investigated its effects on the structures and physical properties of PE membranes. X-ray diffraction data indicated that dipalmitoleoylphosphatidylethanolamine (DPOPE) membranes in H_2O at 20 °C were in the L_α phase and that an L_α to H_{II} phase transition occurred at $X = 0.060$ (mole fraction of DMSO) in water/DMSO mixtures. As the DMSO concentration increased, the basis vector length of the dioleoylphosphatidylethanolamine (DOPE)/16 wt% tetradecane membrane and also of the DPOPE/16 wt% tetradecane membrane in the H_{II} phase decreased, suggesting that the spontaneous curvature of these membranes increased. We have also investigated the effects of DMSO on the physical properties of the PE membranes, and compared them with those of acetone. As the DMSO concentration increased, the excimer to monomer fluorescence intensities of pyrene-phosphatidylcholine in the PE membranes decreased, indicating that the membrane fluidity decreased, and also the generalized polarization value of the Laurdan fluorescent probe in the DPOPE membrane increased, indicating that the polarity of the membrane interface decreased. On the other hand, acetone had the opposite effects to DMSO. The interaction free energy between the membrane surface segments and solvent increased with an increase in DMSO concentration. It decreased the amount of solvent in the membrane interface, inducing an increase in the spontaneous curvature. This can reasonably explain the effects of DMSO on the phase stability and the physical properties of the membranes.

Keywords Dimethyl sulfoxide · Hexagonal II phase · Spontaneous curvature · Phase transition · Interaction free energy

Abbreviations *DEPE*: 1,2-dielaidoyl-*sn*-glycero-3-phosphatidylethanolamine · *DOPE*: 1,2-dioleoyl-*sn*-glycero-3-phosphatidylethanolamine · *DPOPE*: 1,2-dipalmitoleoyl-*sn*-glycero-3-phosphatidylethanolamine · *GP*: generalized polarization · *H_{II} phase*: hexagonal II phase · *L_α phase*: liquid-crystalline phase · *MLV*: multilamellar vesicle · *SAXS*: small-angle X-ray scattering · *WAXS*: wide-angle X-ray scattering

Introduction

Recent new findings have again evoked interest in nonbilayer membranes such as the inverted hexagonal (H_{II}) phase and several kinds of cubic phases, not only because these nonbilayer structures have been postulated to play an important biological role in membrane fusion and control of the functions of membrane proteins (Basáñez et al. 1996; Perkins et al. 1996; de Kruijff 1997; Luzzati 1997; Hayakawa et al. 1998), but also because these nonbilayer membranes have been demonstrated to be useful for crystallization of membrane proteins (Pebay-Peyroula et al. 1997). To elucidate the mechanism of these phenomena, it is essential to understand the mechanism of phase stability, phase transitions

M. Yamazaki (✉)
Department of Physics, Faculty of Science,
Shizuoka University, 836 Oya, Shizuoka 422-8529, Japan
E-mail: spmyama@ipc.shizuoka.ac.jp
Tel.: +81-54-2384741

K. Kinoshita[1] · S.J. Li · M. Yamazaki
Materials Science, Graduate School of Science
and Engineering, Shizuoka University,
Shizuoka 422-8529, Japan

Present address:
[1]c/o Prof. R. Epand,
Department of Biochemistry, McMaster University,
Hamilton, Ontario L8N 3Z5, Canada

between different nonbilayer structures and also between these nonbilayer phases and the liquid-crystalline bilayer (L_α) phase (Fig. 1), and factors determining the size and form of these nonbilayer membranes (Gruner et al. 1985, 1988; Rand and Fuller 1994; Seddon and Templer 1995; Marsh 1996; Luzzati 1997; Aota-Nakano et al. 1999).

On the other hand, the interaction of water with lipid membranes and also the physical properties of the lipid-water interface in biomembranes have been recently considered to play important roles in the stability of lipid vesicles, phase stability, and interactions of biomembranes with various kinds of solutes, and thereby they have been studied by several biophysical techniques and by molecular dynamics simulation (Rand and Parsegian 1989; Yamazaki et al. 1989; Lipowsky 1991; Yamazaki et al. 1992; Ulrich and Watts 1994; Cevc et al. 1995; Chiu et al. 1996; Israelachvili and Wennerström 1996; Sackmann 1996; Tu et al. 1996). However, physical characterization of this lipid-water interface or the interface of biomembranes is still insufficient, and the roles of hydration and water structure in biomembranes are controversial (Israelachvili and Wennerström 1996). To elucidate the essence of the interaction of water with lipid membranes, an investigation of the effects of various kinds of solvents on the structure, phase stability, and intermembrane interactions of lipid membranes is complementary. In this regard, we have proposed that the interaction free energy of the segments of the surface (or interface) of lipid membranes with solvents, ΔG_i (or $\chi = \Delta G_i / k_B T$; a dimensionless parameter), plays an important role in the structure and phase behavior of these membranes (Kinoshita and Yamazaki 1996, 1997; Kinoshita et al. 1997, 1998). ΔG_i is defined as the free energy increase associated with the contact of the segments with the solvent. In good solvents, where the interaction between the segments of the membrane surface and the solvents is favorable (i.e., ΔG_i is small), the segments swell to contact the solvents; on the other hand, in poor solvents, where their interaction is unfavorable (i.e., ΔG_i is large), the segments shrink or associate with each other to prevent contact with the solvents. This new concept can explain reasonably the induction of the interdigitated gel phase ($L_\beta I$ phase) in multilamellar vesicles (MLVs) of dipalmitoylphosphatidylcholine (DPPC) and also the H_{II} to L_α phase transition in the dioleoylphosphatidylethanolamine (DOPE) membrane above critical concentrations of water-miscible organic solvents such as acetone, acetonitrile, and ethanol, and also the intermembrane distance determined by the intermembrane interaction in MLVs (Kinoshita and Yamazaki 1996, 1997; Kinoshita et al. 1998). For the H_{II} to L_α phase transition in DOPE membranes above their critical concentrations, we have proposed a mechanism as follows (Kinoshita and Yamazaki 1997). These water-miscible organic solvents have a high solubility for alkanes, and hence they induce a decrease in the interaction free energy between the solvents and the hydrophobic segments of the alkyl chains in the membrane interface. Thereby, the contact of the alkyl chains with the solvents increases, inducing an increase in the area of the phospholipid headgroups. As a result, the packing parameter of the phospholipid decreases, which increases the stabilization of the L_α phase of the DOPE membrane.

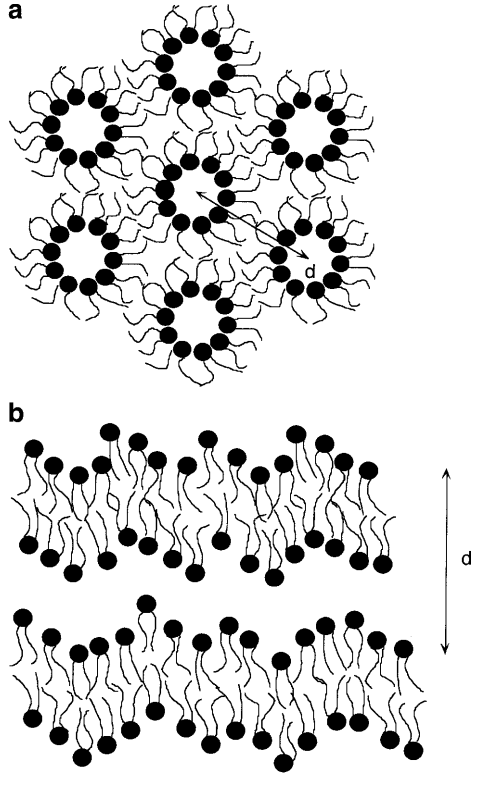

Fig. 1 Schematic representation of H_{II} (**a**) and L_α (**b**) phospholipid phases. Lipid headgroups are represented by *black circles* attached to two hydrocarbon chains

Dimethyl sulfoxide (DMSO) has been used as a cryoprotectant for cells, tissues, and isolated proteins, and also has been known to induce membrane fusions between cells and phospholipid vesicles (Ahkong et al. 1975). Several groups have studied the effects of DMSO on the structure and phase stability of phosphatidylcholine (PC) (Yu and Quinn 1995; Gordeliy et al. 1998; Tristram-Nagle et al. 1998; Smondyrev and Berkowitz 1999). The intermembrane distances of MLVs composed of a PC lipid with a saturated alkyl chain, such as DPPC in the gel phase, decreased with an increase in DMSO concentration, and also the temperatures of the pre and main transitions of these PC-MLVs increased with an increase in DMSO concentration. Recently, it was shown that DMSO decreases the temperature of the L_α to H_{II} phase transition, and thereby stabilizes the H_{II} phase relative to the L_α phase (Yu et al. 1996). However, the mechanisms are not clear yet.

In this report, we have investigated the effects of DMSO on the phase stability of dipalmitoleoylphosphatidylethanolamine (DPOPE) membranes at 20 °C, which is in the L_α phase in water. We have found by small-angle X-ray scattering (SAXS) that an L_α to H_{II}

phase transition occurred at 20 °C at low concentrations of DMSO, indicating that DMSO stabilizes the H_{II} phase rather than the L_α phase under this condition. The SAXS data show that the basis vector length of the DOPE membrane containing 16 wt% tetradecane in excess water decreased with an increase in DMSO concentration, suggesting that the radius of the spontaneous curvature of the DOPE membrane decreased with an increase in DMSO concentration. SAXS data indicated that the DPOPE membrane containing 16 wt% tetradecane at 20 °C was in the H_{II} phase. By using this membrane, we have investigated the effect of DMSO on the spontaneous curvature of the DPOPE membrane, and found a similar result as that for the DOPE membrane. We have also investigated the effects of DMSO on the physical properties of the PE membranes such as the membrane fluidity and the polarity of the membrane interface, and compared them with those for the PE membranes in acetone, which has an opposite effect on the stability of the H_{II} and the L_α phases compared with DMSO. Based on these results, we discuss below the mechanism of the stabilization of the H_{II} phase by DMSO and its effect on the physical properties of the PE membranes.

Materials and methods

Materials

1,2-Dipalmitoleoyl-*sn*-glycero-3-phosphatidylethanolamine (DPOPE), 1,2-dioleoyl-*sn*-glycero-3-phosphatidylethanolamine (DOPE), and 1,2-dielaidoyl-*sn*-glycero-3-phosphatidylethanolamine (DEPE) were purchased from Avanti Polar Lipids. 1-Hexadecanoyl-2-(1-pyrenedecanoyl)-*sn*-glycero-3-phosphatidylcholine (pyrene-PC) and Laurdan were purchased from Molecular Probes. DMSO and acetone were purchased from Wako Chemical. *O*-Phosphorylethanolamine was purchased from Sigma Chemical.

Sample preparations

Several PE membranes were prepared as follows. The appropriate amount of phospholipid in chloroform was dried by N_2, and then under vacuum by rotary pump. The appropriate amount of water containing a given concentration of DMSO was added to this dry lipid in excess solvent (~7 wt% lipids), and the suspension was vortexed for about 30 s at room temperature (~20 °C) several times. For measurement of X-ray diffraction, pellets (or precipitation) of the suspensions after the vortex without centrifugation were used.

To investigate the structures of DOPE and DPOPE membranes containing 16 wt% tetradecane (see Fig. 5 below), we used almost the same method as Chen and Rand (1997, 1998) as follows. The appropriate amount of DOPE or DPOPE in chloroform was dried by N_2, and then under vacuum by rotary pump for more than 12 h. Tetradecane was added to the dry lipid by weighing directly. After 48 h incubation at room temperature (~25 °C) for equilibration, the appropriate amount of water containing a given concentration of DMSO was added to this dry-lipid/tetradecane mixture in excess solvent (~7 wt% lipids), and the suspension was vortexed for about 30 s at room temperature (~25 °C) several times, and then incubated for another 48 h for equilibration. For X-ray diffraction measurements, pellets (or precipitation) of the suspensions after the vortex without centrifugation were used.

To determine the dimensions of the phospholipid membranes in the H_{II} and L_α phases (see Fig. 10 below), the phospholipids were solvated by weighing the dry lipid and solvent into an aluminum pan (vessel for liquid samples for the DSC experiment), which was sealed completely and then equilibrated at room temperature for 2 days (in the case of water) or 2–5 days (in the case of DMSO/water mixtures). After the equilibration, the samples were sealed in a thin-walled glass capillary tube (outer diameter 1.0 mm) for X-ray diffraction.

X-ray diffraction

X-ray diffraction experiments were performed using nickel-filtered Cu K_α X-rays ($\lambda = 0.154$ nm) from a rotating anode-type X-ray generator (Rigaku, Rotaflex, RU-300, 40 kV × 200 mA). SAXS data were recorded using a linear (one-dimensional) position-sensitive proportional counter (Rigaku, PSPC-5) (Glatter and Kratky 1982) with a camera length of 350 mm and analyzed by a multichannel analyzer (Rigaku) and a computer. Wide-angle X-ray scattering (WAXS) patterns were recorded by a flat plate film cassette loaded with a high-sensitive X-ray film (Fuji Medical X-ray film) with a camera length of 45.1 mm. Samples were sealed in a thin-walled glass capillary tube (outer diameter 1.0 mm) and mounted in a thermostatable holder whose stability was ±0.2 °C (Yamazaki et al. 1992).

To determine the dimensions of phospholipid membranes in the H_{II} and L_α phases, the technique developed by Luzzati was used (Luzzati and Husson 1962). For the membranes in the H_{II} phase, the basis vector length (i.e., center to center distance of adjacent cylinders defined in Fig. 1), d, calculated by $d = (2/\sqrt{3})x$ (where x is the spacing in the SAXS), is expressed as a sum of the radius of the water tube, R_w, and the thickness of the monolayer membrane, d_l, i.e., $d = 2(R_w + d_l)$ (Gruner 1985; Tate and Gruner 1989). R_w is calculated by the volume fraction of lipid, ϕ_L, and the basis vector length d as follows:

$$R_w = d\sqrt{(1-\phi_L)\sqrt{3}/2\pi} \tag{1}$$

For the membranes in the L_α phase, the area per lipid molecule, A^{bil}, is calculated by the volume fraction of lipid, ϕ_L, and the spacing d (Fig. 1) (Rand and Fuller 1994) as follows:

$$A^{bil} = 2(V_w + V_L)/d = 2V_L/d\phi_L \tag{2}$$

where V_L is the volume of one phospholipid molecule, and V_w is the volume of water per phospholipid molecule.

Volume fractions of the phospholipids (ϕ_L) were determined by their weight fractions (ϕ_L(w/w)) and the density of the phospholipids and water. The densities of DOPE in the H_{II} phase and DPOPE in the L_α phase were determined by a neutral buoyancy technique (Nagle and Wilkinson 1978; Tate and Gruner 1989). Phospholipids added to H_2O/D_2O mixed solvents of different ratios were centrifuged at each temperature, and the density of the H_2O/D_2O mixed solvent where the lipid becomes buoyant was obtained. This method yielded a density of phospholipid (ρ_L) for DOPE at 20 °C of 1.017 g/mL, which was almost the same value reported by another group (Tate and Gruner 1989), and also a density (ρ_L) for DPOPE at 20 °C of 1.035 g/mL. Volume fractions of the phospholipids (ϕ_L) were determined by their weight fractions (ϕ_L(w/w)) according the following equation:

$$\phi_L = \frac{\frac{\phi_L(w/w)}{\rho_L}}{\frac{\phi_L(w/w)}{\rho_L} + \frac{(1-\phi_L(w/w))}{\rho_W}} \tag{3}$$

where ρ_W is a density of water at 20 °C (ρ_W = 0.998 g/mL).

Differential scanning calorimeter

DSC experiments were performed using a Rigaku DSC-8230-B instrument. A DEPE-MLV dispersion (1.4 wt% lipid) was heated at a rate of 2.0 °C/min. The main transition temperature (the chain-melting transition temperature) was determined as the onset of the

endothermic transition extrapolated to the baseline. The details were described in our previous paper (Yamazaki et al. 1992).

Fluorescence measurements

For fluorescence measurements, a Hitachi F3000 spectrofluorimeter was used. Fluorescence intensities of the samples were measured at 20 ± 0.5 °C using a circulator (Refrigerated Circulator, RTE-110, NES-LAB) (Kinoshita and Yamazaki 1996).

Fluorescence measurement of pyrene-PC

The excitation wavelength of pyrene-PC was 347 nm, and emission wavelengths were 376 nm for monomer fluorescence and 481 nm for excimer fluorescence. Excitation bandpass and emission bandpass were 3 nm and 1.5 nm, respectively. The pyrene-PC concentration in the total phospholipids was 5.0 mol%. At 30 min after mixing the phospholipid dispersions with DMSO solution, fluorescence intensities of samples were measured at 20 °C. Fluorescence intensities were obtained by their time averaging for 30 s, and by using these values the ratio of excimer to monomer fluorescence intensities (E/M) was calculated. The concentrations of the total phospholipids in the samples for the measurement of the fluorescence were 70–80 μM, which were determined by standard phosphate analysis (Bartlett 1959).

Fluorescence measurement of Laurdan

To investigate the effect of DMSO and acetone on the polarity of the phospholipid interface, we used an amphiphilic fluorescence probe, Laurdan, which is considered to locate at the hydrophilic-hydrophobic interface of bilayers with the lauric acid tail anchored in the hydrophobic zone of the membrane (Parasassi et al. 1991). The excitation wavelength of Laurdan was 340 nm; excitation bandpass and emission bandpass were 5 nm and 5 nm, respectively. The concentration of Laurdan in the total lipids was 0.30 mol%. Concentrations of the total phospholipids in the samples for the measurement of the fluorescence were 70–80 μM, which were determined by standard phosphate analysis (Bartlett 1959). At 30 min after mixing the phospholipid dispersions with the DMSO solution, fluorescence intensities of the samples were measured at 20 °C. Fluorescence intensities for calculation of generalized polarization (GP) values were obtained by their time averaging for 10 s.

Measurement of solubility

Measurement of the solubility of a molecule having the same structure as the headgroup of phospholipids was done by the same method described in a previous paper (Kinoshita et al. 1997).

Appropriate amounts of *O*-phosphorylethanolamine were mixed with various concentrations of aqueous DMSO solutions in order to make saturated solutions, and centrifuged. Concentrations of phosphorylethanolamine in the supernatant of these solutions were determined by standard phosphorus analysis (Bartlett 1959).

Results

Interaction of DMSO with DOPE membranes

In a previous paper (Kinoshita and Yamazaki 1997), we indicated that several water-miscible organic solvents, such as acetone, acetonitrile, and ethanol, induced the H_{II} to L_α phase transition in a DOPE membrane above their threshold concentrations, and stabilized the L_α phase relative to the H_{II} phase. These organic solvents have high solubilities for alkanes. As a control experiment, we have investigated the effects of DMSO, which has a low solubility for alkanes and for which the oil-water partition coefficient is low (Bunch and Edwards 1969), on the phase behavior and structure of DOPE membranes by X-ray diffraction. SAXS data of the DOPE membrane in excess water at 20 °C showed that a set of SAXS peaks had spacings in the ratio of $1:\sqrt{3}:2:\sqrt{7}$, indicating that it was in a two-dimensional hexagonal (H_{II}) phase (Kirk and Gruner 1985; Seddon and Templer 1995). In the presence of various DMSO concentrations up to 0.28 mole fraction of DMSO in water/DMSO mixtures ($X_{DMSO} = 0.28$), the ratios of the SAXS spacings were not changed, and thus the membranes were in the H_{II} phase. The basis vector length of the H_{II} phase (center to center distance of adjacent cylinders), d, calculated by $d=(2/\sqrt{3})x$ (where x is the spacing in the SAXS) (Fig. 1), gradually decreased from 7.6 nm to 4.9 nm with an increase in DMSO concentration from $X_{DMSO} = 0$ to $X_{DMSO} = 0.28$ (Fig. 2).

For comparison, SAXS data for the DOPE membranes in various concentrations of acetone at 20 °C are shown in Fig. 2 (Kinoshita and Yamazaki 1997). At 0.035 mole fraction of acetone in a water/acetone mixture ($X_{acetone}=0.035$), a new set of SAXS peaks with a shorter spacing was superimposed on the H_{II} peaks; the new set had spacings in the ratio of 1:2:3, which is consistent with an L_α phase. Therefore, the H_{II} to L_α phase transition in DOPE membranes occurred at $X_{acetone}=0.035$.

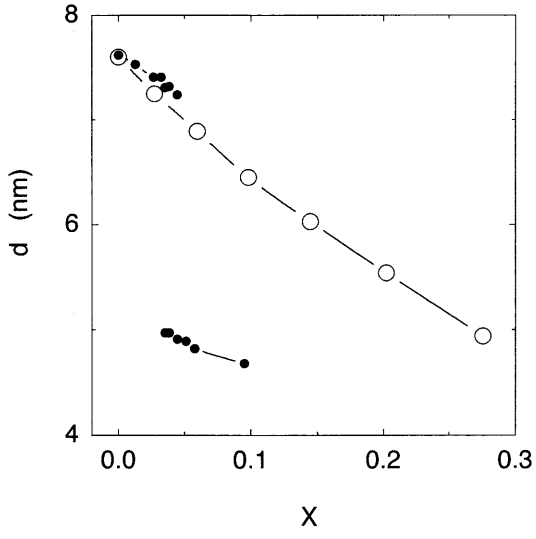

Fig. 2 The structure parameter, d, of the DOPE membrane in various concentrations of DMSO [in mole fraction of DMSO in water/DMSO mixtures (X_{DMSO})] (○) and acetone [in mole fraction of acetone in water/acetone mixtures ($X_{acetone}$)] (●) at 20 °C. In the data points for acetone (●), the upper points ($0 < X_{acetone} < 0.05$) represent the H_{II} phase, while the lower points ($0.35 \leq X_{acetone} < 0.1$) represent the L_α phase. The structure parameter d is both the basis vector length for the H_{II} phase and the spacing for the L_α phase, which is defined in Fig. 1

Interaction of DMSO with DPOPE membranes

Next, we have investigated by X-ray diffraction the effects of DMSO on the phase behavior and structure of DPOPE membranes. The DPOPE membrane in excess water at 20 °C is known to be in the L_α phase (Colotto et al. 1996). Figure 3 shows SAXS patterns of the DPOPE membranes at $X_{DMSO}=0$, 0.082, and 0.12 at 20 °C. The DPOPE membrane in water showed a set of SAXS peaks with spacings in the ratio of 1:2:3 and the spacing was 4.9 nm (Fig. 3a). A WAXS pattern of this DPOPE membrane consisted of a diffuse broad band around 0.46 nm. These results indicate that it was in the L_α phase. At $X_{DMSO}=0.12$, a set of SAXS peaks had spacings in the ratio of 1:√3:2:√7, indicating that it was in the H_{II} phase (Fig. 3c). At $X_{DMSO}=0.082$, both the peaks due to the L_α phase and the H_{II} phase appeared in the SAXS pattern (Fig. 3b), indicating that the phases coexisted. Figure 4 shows a detailed dependence of the spacing on DMSO concentration. Below $X_{DMSO}=0.060$, the SAXS patterns of the DPOPE membranes had similar sets of peaks as at $X_{DMSO}=0$, and thus they were in the L_α phase. This spacing gradually decreased with an increase in DMSO concentration. Above $X_{DMSO}=0.060$, a new set of SAXS peaks with a larger spacing was superimposed on the L_α peaks; the new set had spacings in the ratio of 1:√3:2:√7, which is consistent with a H_{II} phase. The basis vector length of the H_{II} phase, d, gradually decreased from 6.8 nm to 5.5 nm with an increase in DMSO concentration from $X_{DMSO}=0.060$ to $X_{DMSO}=0.20$ (Fig. 4). Hence, DMSO induced a phase transition from the L_α to the H_{II} phase in the DPOPE dispersion at $X_{DMSO}=0.060$.

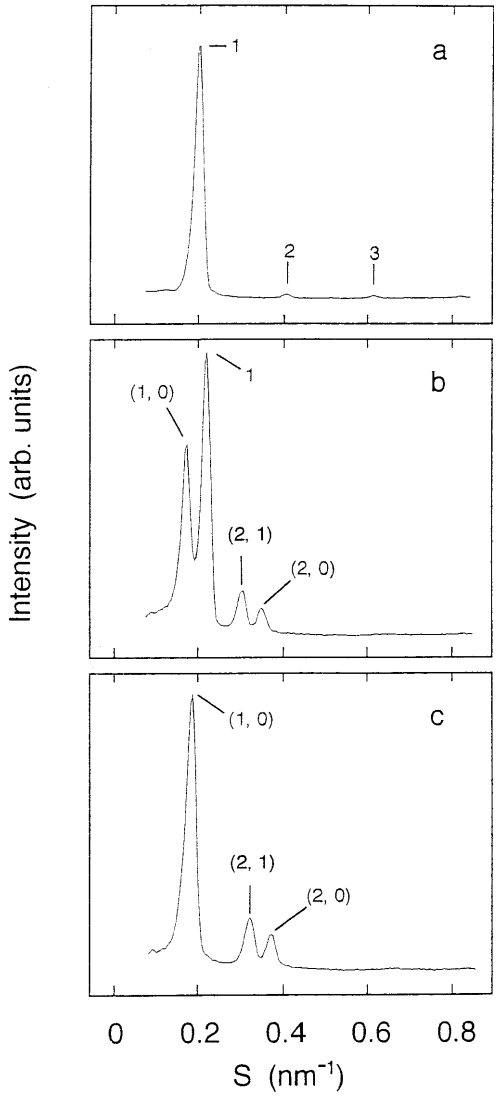

Fig. 3 X-ray diffraction profile of the DPOPE membrane in various concentrations of DMSO, X_{DMSO}, in water at 20 °C: **a** $X_{DMSO}=0$, **b** 0.082, **c** 0.12

Interaction of DMSO with DOPE/tetradecane and DPOPE/tetradecane membranes

To allow the lipid membranes in the H_{II} phase to express the spontaneous curvature, H_0, the addition of alkanes such as decane and tetradecane to the membranes is required because they fill the interstitial region of the H_{II} phase and relax the alkyl chain-packing stress (Gruner 1985; Rand et al. 1990; Chen and Rand 1998). Thereby, to obtain information on the dependence of the spontaneous curvature of the DOPE membrane on DMSO concentration, we have investigated the structure of DOPE membranes containing 16 wt% tetradecane (Chen and Rand 1997) in the presence of various concentrations of DMSO (Fig. 5). The basis vector length d

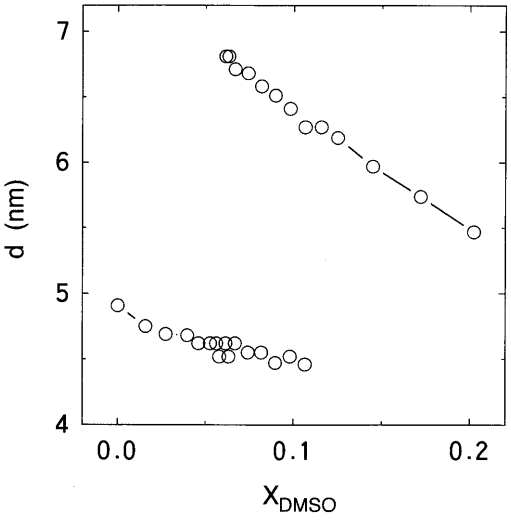

Fig. 4 The structure parameter d of the DPOPE membrane in various concentrations of DMSO, X_{DMSO}, in H_2O (○) at 20 °C. In the data points the lower points ($0 \le X_{DMSO} < 0.11$) represent the L_α phase, while the upper points ($0.06 < X_{DMSO} < 0.21$) represent the H_{II} phase. The structure parameter d is both the basis vector length for the H_{II} phase and the spacing for the L_α phase, which is defined in Fig. 1

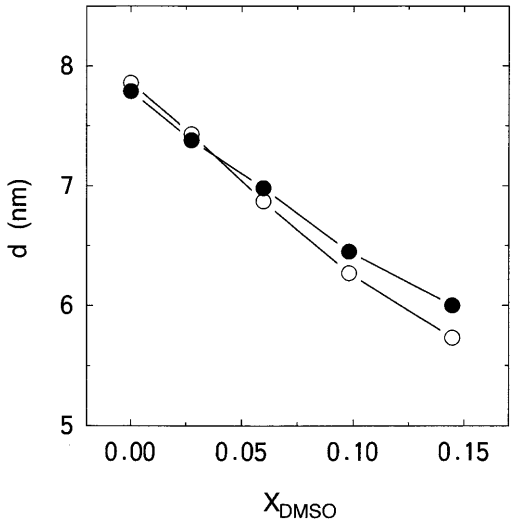

Fig. 5 Basis vector length d of the DOPE/tetradecane (○) and DPOPE/tetradecane (●) membranes in various concentrations of DMSO, X, in water at 20 °C. All the membranes were in the H_{II} phase irrespective of DMSO concentration. The basis vector length of the H_{II} phase is defined in Fig. 1

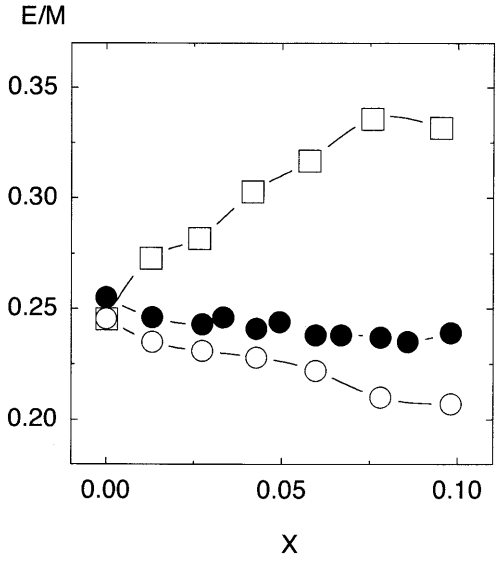

Fig. 6 Ratio of excimer to monomer fluorescence intensities (E/M) of pyrene-PC in the DPOPE membrane (●) and in the DOPE membrane (○) in various concentrations of DMSO (X_{DMSO}), and E/M of pyrene-PC in the DOPE membrane (❑) in various concentrations of acetone ($X_{acetone}$) at 20 °C. The size of the symbols shows the error of the measured E/M values. The pyrene-PC concentration in the total phospholipids was 5.0 mol%

of the DOPE/tetradecane membrane in excess water gradually decreased from 7.9 nm to 5.7 nm with an increase in DMSO concentration from $X_{DMSO}=0$ to $X_{DMSO}=0.14$.

We have also investigated the structure of DPOPE membranes containing 16 wt% tetradecane in the presence of various concentrations of DMSO (Fig. 5). In water only (i.e., $X_{DMSO}=0$), the pure DPOPE membrane was in the L_α phase (Fig. 3), but the DPOPE membrane containing 16 wt% tetradecane was in the H_{II} phase with a basis vector length d of 7.8 nm. As shown in Fig. 5, d of the DPOPE/tetradecane membrane in excess water gradually decreased from 7.8 nm to 6.0 nm with an increase in DMSO concentration from $X_{DMSO}=0$ to $X_{DMSO}=0.14$.

Fluidity change of the PE membranes induced by DMSO and acetone

The results of Fig. 2 and Fig. 4 clearly indicate that DMSO stabilizes the H_{II} phase relative to the L_α phase, but, on the other hand, acetone stabilizes the L_α phase relative to the H_{II} phase. To make clear the different effects of DMSO and acetone on the PE membranes, we have investigated the effects of these organic solvents on the physical properties of the PE membranes.

At first, to investigate the effect of DMSO and acetone on the membrane fluidity, we measured the lateral diffusion of the phospholipid in the PE membranes in various concentrations of DMSO and acetone, using an excimer-forming fluorescent probe, pyrene-PC. The ratio of the excimer to monomer fluorescence intensity (E/M) of pyrene-PC in membranes is proportional to the collision frequency of pyrene molecules (Galla et al. 1979; Galla and Hartmann 1980) and, especially in the liquid-crystalline phase, a lateral diffusion coefficient of the membrane, D, can be determined by E/M, and D increases with an increase in E/M (Galla and Hartmann 1980; Sassaroli et al. 1990). Figure 6 shows that E/M of the DPOPE and DOPE membranes at 20 °C decreased with an increase in DMSO concentration; on the other hand, E/M of the DOPE membranes at 20 °C increased with an increase in acetone concentration.

Change of Laurdan fluorescence behavior in the DPOPE membrane induced by DMSO and acetone

To investigate the effect of DMSO and acetone on the polarity of the lipid interface, we used an amphiphilic fluorescence probe, Laurdan. The emission spectrum of this probe is strongly dependent on its surroundings, and in solvents with high polarity the spectra show a large red shift due to the dipolar relaxation process (Parasassi et al. 1991; Bagatolli et al. 1998). In phospholipid membranes, at the gel phase an emission maximum is around 440 nm, and at the liquid-crystalline phase it is around 490 nm, indicating that the emission spectrum of Laurdan largely depends on the packing of the phospholipid alkyl chains, which is one of the main determinants of the number and motional freedom of water molecules around the fluorescent group. The generalized polarization (GP) value $[=(I_B - I_R)/(I_B + I_R)]$ for phospholipid vesicles at emission wavelengths of 440 nm (for I_B) and 490 nm (for I_R) is strongly affected by the polarity of the membrane interface, and it

rapidly decreases when a gel to liquid-crystalline phase transition occurs (Parasassi et al. 1991). Figure 7 shows that the GP value for DPOPE-MLVs at 20 °C increased with an increase in DMSO concentration, whereas it decreased with an increase in acetone concentration.

Effects of DMSO and acetone on the chain-melting phase transition temperature of DEPE membranes

We have investigated the effects of DMSO or acetone on the phase transition temperature, T_m, from the gel to the liquid-crystalline phase of DEPE membranes. As shown in Fig. 8, T_m increased with an increase in DMSO concentration, but decreased with an increase in acetone concentration.

Solubility of phosphorylethanolamine

To obtain information about the free energy of the interaction between the hydrophilic segments of these PE membranes with solvents, we have investigated the dependence of the solubility of phosphorylethanolamine on DMSO concentration in DMSO/water mixtures by the same method as applied to the PC membrane (Kinoshita et al. 1997, 1998). The phosphorylethanolamine molecule has the same molecular structure as the head group of PE, and thereby it represents a hydrophilic segment of the membrane interface of these PE membranes. Figure 9 shows that the solubility of phosphorylethanolamine in water at 20 °C decreased with an increase in DMSO concentration. This result indicates that DMSO is a poor solvent for the hydrophilic segments of the PE membrane, and the interaction free energy between the solvent and the hydrophilic segments of the PE membrane increases with an increase in DMSO concentration.

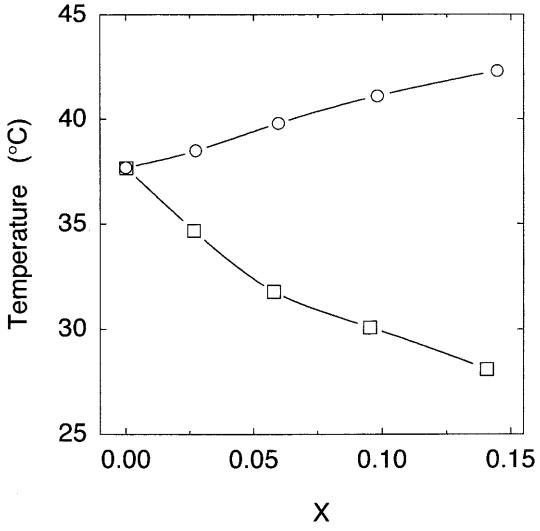

Fig. 8 Chain-melting phase transition temperature of the DEPE membrane in various concentrations of DMSO (X_{DMSO}) (○) and acetone ($X_{acetone}$) (❑) determined by DSC. Heating rate was 2.0 K/min. The transition temperatures were determined as the onset of the endothermic transition extrapolated to the baseline

Effect of water content on the structure and phase behavior of DPOPE membranes

Figure 10 shows the basis vector length d of the DOPE and the spacing d of the DPOPE membranes at 20 °C

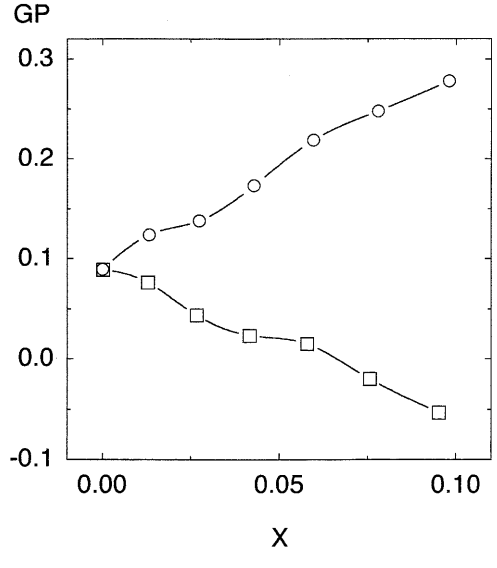

Fig. 7 Generalized polarization value (GP) for Laurdan in the DPOPE membrane in various concentrations of DMSO (X_{DMSO}) (○) and in various concentrations of acetone ($X_{acetone}$) (❑) at 20 °C. The concentration of Laurdan in the total phospholipids was 0.30 mol%

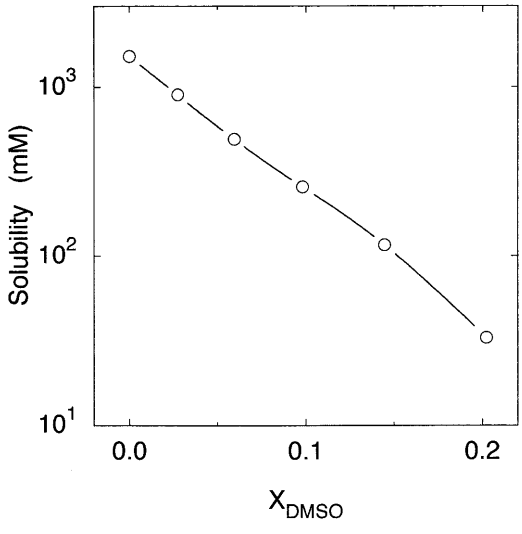

Fig. 9 Solubility of phosphorylethanolamine (○) in various concentrations of DMSO (X_{DMSO}) in DMSO/water mixtures at 20 °C. The solubility was measured as described in Materials and methods

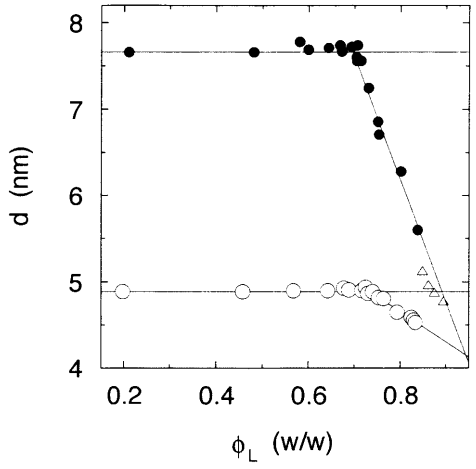

Fig. 10 The points ● show the basis vector length, d, of the H_{II} phase of DOPE as a function of lipid weight fraction, ϕ_L(w/w), at 20 °C. The points ○ and Δ show the spacing d of the L_α phase and the basis vector length d of the H_{II} phase of the DPOPE membrane as a function of lipid weight fraction, ϕ_L(w/w), at 20 °C, respectively

as a function of the weight fraction (w/w) of the phospholipid. A sharp reduction in d was observed above the critical values of the lipid weight fraction [ϕ_L(w/w)* = 0.695 for the DOPE membrane and ϕ_L(w/w)* = 0.734 for the DPOPE membrane]. In the case of the DPOPE membrane, on increasing the lipid weight fraction, at ϕ_L(w/w) = 0.85 a phase transition from the L_α to the H_{II} phase occurred. The equilibrium basis vector length d of the DOPE membrane was 7.6 nm, and the equilibrium spacing d of the DPOPE membrane was 4.9 nm. In the case of the DOPE membrane, the radius of the water core of the H_{II} phase, R_w, was determined to be 2.2 nm, and in the case of the DPOPE membrane the area per lipid molecule in the L_α phase, A^{bil}, was determined to be 62 Å^2 from these critical values [ϕ_L(w/w)*]. We tried to obtain d as a function of lipid weight fraction (w/w) of the DOPE in the presence of DMSO such as $X_{DMSO} = 0.060$ and 0.098, but could not obtain a conclusive result owing to the difficulty in attaining the equilibrium.

Discussion

In a previous paper (Kinoshita and Yamazaki 1997), we indicated that type A solvents, i.e., several water-miscible organic solvents such as acetone, acetonitrile, and ethanol, induced the H_{II} to L_α phase transition in the DOPE membranes above their critical concentrations, and stabilized the L_α phase relative to the H_{II} phase. On the other hand, the results of the X-ray diffraction in this report and in other reports (Yu and Quinn 1995; Yu et al. 1996) clearly indicate that DMSO stabilizes the H_{II} phase relative to the L_α phase in several PE membranes. Hence, DMSO has the opposite effect on the PE membranes compared with type A solvents. What kind of factor is important for this different effect? Especially, in type A solvents, acetone $(CH_3)_2C{=}O$ has a similar chemical structure as DMSO $(CH_3)_2S{=}O$; the difference is just a carbon atom replacing a sulfur atom. Therefore, it is valuable to compare the effects of these solvents on the physical properties of the PE membranes. Figure 6 clearly shows that the fluidity of the PE membranes decreased with an increase in DMSO concentration, whereas it largely increased with an increase in acetone. Figure 7 shows that the GP value of Laurdan increased with an increase in DMSO concentration, suggesting that the polarity of the membrane interface decreased. On the other hand, the effect of acetone on the interface is the reverse: the polarity increased with an increase in acetone concentration. These results show the completely opposite effects of DMSO and acetone on the physical properties of the PE membranes. What causes these differences, and how do they relate to the different effects of DMSO and acetone on the phase stability of the PE membranes?

The mechanism of the L_a to H_{II} phase transition of PE membranes induced by DMSO

The difference of the chemical potential of the phospholipid in the membranes in the H_{II} phase (μ^{HII}) and in the bilayer liquid-crystalline (L_α) phase (μ^{bil}), $\Delta\mu$, is expressed as follows (see e.g. Gruner 1985; Anderson et al. 1988):

$$\begin{aligned}\Delta\mu &= \mu^{HII} - \mu^{bil} \\ &= \left(\mu^{HII}_{curv} - \mu^{bil}_{curv}\right) + \left(\mu^{HII}_{ch} - \mu^{bil}_{ch}\right) + \left(\mu^{HII}_{hd} - \mu^{bil}_{hd}\right) \\ &= \Delta\mu_{curv} + \Delta\mu_{ch} + \Delta\mu_{hd} \qquad (4)\end{aligned}$$

where $\Delta\mu_{curv}$ is a term due to the curvature elastic energy (or curvature energy), $\Delta\mu_{ch}$ is a term due to interstitial chain packing of the H_{II} phase, and $\Delta\mu_{hd}$ is a term due to the membrane interface. Other groups have presented a similar expression (Kozlov et al. 1994). The spontaneous (or intrinsic) curvature of a single monolayer membrane, H_0, is a useful parameter characterizing nonbilayer membranes, and expressed as $H_0 = 1/R_0$, where R_0 is the radius of spontaneous curvature (Gruner 1985; Hui and Sen 1989; Tate and Gruner 1989; Marsh 1996). Inverted curved structures such as the H_{II} phase, where the spontaneous curvature of the monolayer is toward the water region, have large negative H_0 values; on the other hand, normal structures such as micelles, where the spontaneous curvature of the monolayer is toward the alkyl chain region, have large positive H_0 values. As the repulsive interaction between the headgroups owing to electrostatic interaction or steric interaction increases, the absolute value of H_0 decreases to increase the average area of the lipid headgroup. On the other hand, the decrease in the repulsive interaction increases the absolute value of H_0. By using R_0, the curvature energy of the H_{II} phase and the L_α phase, μ_{curv} in Eq. (4), is expressed as (Kirk et al. 1984; Marsh 1996):

$$\mu_{curv} = \frac{1}{2}(N_A \kappa A o)\left(\frac{1}{R_w} - \frac{1}{R_0}\right)^2 \quad (5)$$

where N_A is Avogadro's number, κ is the elastic bending modulus, A_o is the optimal surface area per lipid molecule in the membrane, R_w is the radius of curvature of the lipid monolayer. In excess water, the membrane in the H_{II} phase has a curvature close to the spontaneous curvature to minimize the curvature energy, and thereby $R_w \approx R_0$. For convenience, we define $\mu_{curv}^{HII} = 0$ in excess water. Since $1/R_w = 0$ in the L_α phase:

$$\Delta\mu_{curv} = \left(\mu_{curv}^{HII} - \mu_{curv}^{bil}\right) = -\frac{1}{2}\frac{N_A \kappa A_o^{bil}}{R_0^2} \quad (<0) \quad (6)$$

where A_o^{bil} is the optimal surface area per lipid molecule of the L_α phase. Equation (6) shows that $\Delta\mu_{curv}$ is always negative ($\Delta\mu_{curv} < 0$), and thereby is an important factor stabilizing the H_{II} phase. On the other hand, in the H_{II} phase, alkyl chains of lipids have to extend to different lengths to fill the interstitial hydrocarbon region, which decreases the entropy of the chains and thereby increases the free energy of the membrane (Anderson et al. 1988). Therefore, this packing energy of the alkyl chains destabilizes the H_{II} phase, and thus $\Delta\mu_{ch}$ is always positive ($\Delta\mu_{ch} > 0$). In most cases, phase transitions between the H_{II} and the L_α phases are determined by the interplay of these two factors, $\Delta\mu_{curv}$ and $\Delta\mu_{ch}$. The third term in Eq. (4), the difference in the chemical potential of the membrane interface μ_{hd}, is determined mainly by interactions between the headgroups of the phospholipids and hydrophobic interaction.

Equation (6) shows that the absolute value of $\Delta\mu_{curv}$ increases with a decrease in R_0, and the change in the spontaneous curvature induces the change in the curvature energy, $\Delta\mu_{curv}$, as follows:

$$\delta\Delta\mu_{curv} = -\frac{N_A \kappa A_o^{bil}}{R_0}\delta\left(\frac{1}{R_0}\right) \quad (7)$$

The result of Fig. 5 gives information on the change of the radius of spontaneous curvature R_0 of the DOPE and DPOPE membranes. The basis vector length of the H_{II} phase, d, is expressed as a sum of the radius of the water tube, R_w, and the thickness of the monolayer membrane, d_l, i.e., $d = 2(R_w + d_l)$ (Gruner 1985; Tate and Gruner 1989). In excess water, the DOPE membrane containing 16 wt% tetradecane in the H_{II} phase has a curvature close to H_0 to minimize the curvature free energy, and thereby $R_w \approx R_0$ (Chen and Rand 1997). We also found that the DPOPE membrane containing 16 wt% tetradecane was in the H_{II} phase. The tetradecane-induced L_α to H_{II} phase transition in the DPOPE membrane is due to the decrease in $\Delta\mu_{ch}$, because tetradecane can fill the interstitial region of the H_{II} phase and relax the alkyl chain packing stress. Thereby, the above analysis can apply to the DPOPE membrane. The decrease in d of the DOPE/tetradecane and DPOPE/tetradecane membranes induced by DMSO is attributed to the decrease in R_w, since the change in d_l is assumed to be small. This is a similar phenomenon as the decrease in d of the DOPE membrane with an increase in temperature (Tate and Gruner 1989). Thus, the result of Fig. 5 indicates that R_0 of the DOPE and DPOPE membranes decreases with an increase in DMSO concentration, and thereby the absolute value of $\Delta\mu_{curv}$ ($\Delta\mu_{curv} < 0$) increases with an increase in DMSO concentration. Both $\Delta\mu_{ch}$ and $\Delta\mu_{hd}$ do not change significantly with an increase in DMSO concentration. Therefore, the DMSO-induced L_α to H_{II} phase transition can be explained mainly by the change of $\Delta\mu_{curv}$ as a function of DMSO concentration. In water and at lower concentrations of DMSO, $\Delta\mu > 0$, and thereby the L_α phase is stable, but $\Delta\mu$ decreases with an increase in DMSO concentration owing to the increase of the absolute value of $\Delta\mu_{curv}$. At the critical concentration of DMSO, $\Delta\mu = 0$ and the L_α to H_{II} phase transition occurs. Above the critical concentration of DMSO, $\Delta\mu < 0$ and thereby the H_{II} phase is stable. Hence, the decrease in the radius of the spontaneous curvature, R_0, with an increase in DMSO concentration induces the L_α to H_{II} phase transition in the PE membrane.

The mechanism of the decrease in the radius of the spontaneous curvature (R_0) of the PE membranes induced by DMSO

Recently, we have proposed that the interaction free energy of the segments of the surface of phospholipid membranes with solvents, ΔG_i, plays an important role in structure and phase behavior of these membranes (Kinoshita and Yamazaki 1996, 1997; Kinoshita et al. 1997, 1998). ΔG_i is defined as the free energy increase associated with the contact of segments with solvent. In good solvents, where the interaction between the segments of the membrane surface and the solvents is favorable (i.e., ΔG_i is small), the segments swell to contact the solvents; on the other hand, in poor solvents, where their interaction is unfavorable (i.e., ΔG_i is large), the segments shrink or associate with each other to prevent contact with the solvents. Current physical investigations of phospholipid membranes clearly show that their interfaces have dynamic structures and consist of a complex and thermally disordered mixture of the hydrophilic segments of the head group, hydrophobic segments of alkyl chains, and water molecules, because of large thermal fluctuations such as the protrusion of phospholipids and the undulation of the membrane (Helflich 1978; Lipowsky 1991; Israelachvili 1992; Wiener and White 1992; Nagle et al. 1996; Sackmann 1996). Therefore, we have to consider two kinds of segments of the membrane surface, and thereby two kinds of interaction free energy between the surface segments of the phospholipid membrane and solvents: one is a free energy of interaction between the hydrophilic segments of the head groups and solvents (ΔG_{i1}), and the other is a free energy of interaction between the

hydrophobic segments of the alkyl chains and solvents (ΔG_{i2}). This new concept can explain reasonably the induction of the interdigitated gel phase ($L_\beta I$ phase) in DPPC-MLVs and also the H_{II} to L_α phase transition in the DOPE membrane by water-miscible organic solvents such as acetone, acetonitrile, and ethanol, and also the intermembrane distance in MLVs (Kinoshita and Yamazaki 1996, 1997; Kinoshita et al. 1998).

DMSO has a low solubility for alkanes such as hexane [2% (v/v) hexane completely dissolved in DMSO] at 20 °C and the oil-water partition coefficient of DMSO is low (0.0030) (Bunch and Edwards 1969). Several investigations have shown that a DMSO molecule strongly interacts with two water molecules by hydrogen bonding at low concentrations around 20 °C, and thereby DMSO has an effect of rigidifying the water structure, whereas at higher concentrations, DMSO breaks the water structure (Vaismann and Berkowits 1992, and references therein). In this paper, we have investigated the effects of low concentrations of DMSO in water at 20 °C, where the property of DMSO is the former. The DMSO molecule associated with water molecules may have more hydrophilic character than DMSO itself, and thereby it is a poorer solvent for alkanes than DMSO itself. Therefore, ΔG_{i2} of the hydrophobic segments of the membrane interfaces with DMSO at low concentrations in water is large. On the other hand, the type A solvents such as acetone have a high solubility for alkanes and ΔG_{i2} of the hydrophobic segments of the membrane interfaces with these solvents is small (Kinoshita and Yamazaki 1996). Moreover, the result of Fig. 9 indicates that DMSO is a poor solvent for phosphorylethanolamine, which has the same structure of the head group segments of the PE membranes. This result means that DMSO is a poor solvent for the hydrophilic segments of the surface of the PE membranes, and also that ΔG_{i1} of the hydrophilic segments of the PE with solvents increases with an increase in DMSO concentration. Hence, DMSO is a poor solvent for both the hydrophilic segment and hydrophobic segment of the PE membrane surface under this condition (low concentration of DMSO at 20 °C). The increase in ΔG_i induces the shrinkage of the membrane interface consisting of the surface segments and solvents, which decreases the amount of solvents in the membrane interface, and thereby it reduces the effective cross-sectional area of the phospholipid headgroup regions, or induces a conformational change of the hydrophilic segments. The result of the GP value for Laurdan (Fig. 7), indicating that the polarity of the membrane interface decreases with an increase in DMSO concentration, supports the mechanism described above.

Marsh (1996) has shown that H_0 can be expressed in terms of the packing parameter (V/Al) of the whole phospholipid molecule, where V is the average volume of the entire lipid molecule, l is its average length, and A is the average area of the lipid headgroup at the lipid-water interface (Fig. 11), and that in the inverted curved structures, absolute values of H_0 increase (i.e., R_0 decrease) with an increase in V/Al. As described above, the area of the lipid headgroup decreases with an increase in DMSO concentration while V and l are almost constant, and thereby the packing parameter (V/Al) increases with an increase in DMSO concentration. This is why R_0 of the PE membrane decreases (i.e., the absolute value of H_0 increases) with an increase in DMSO.

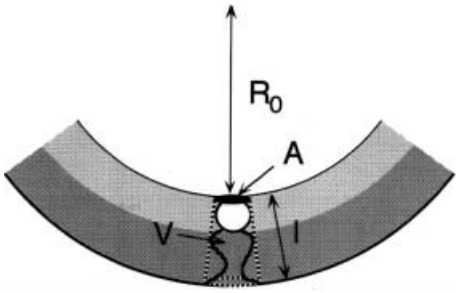

Fig. 11 Topology of the inverted curved lipid monolayer. R_0 is the radius of intrinsic curvature, V is the average volume of the entire lipid molecule, l is its average length, and A is the average area of the lipid headgroup at the lipid-water interface (Marsh 1996)

The shift of the L_α to H_{II} phase transition temperature, ΔT_h, resulting from any external effects can be obtained by Eq. (7) as follows (Marsh 1996):

$$\Delta T_h = \frac{\delta \Delta \mu}{\Delta S_h} = \frac{\delta \Delta \mu_{curv}}{\Delta S_h} = -\frac{1}{2}\left(\frac{N_A \kappa A_o^{bil}}{\Delta S_h}\right)\delta\left(\frac{1}{R_0^2}\right) \propto -\delta\left(\frac{V}{Al}\right) \tag{8}$$

where ΔS_h is the entropy change at the L_α to H_{II} phase transition. At the derivation of Eq. (8), any possible change of the bending elastic modulus, κ, is assumed to be negligible. According to this analysis (Eq. 8), the dependence of ΔT_h on the packing parameter is that $\Delta T_h \propto -\delta(V/Al)$, indicating that an increase in the packing parameter decreases T_h. Thus, the increase in the packing parameter with an increase in DMSO concentration induces a decrease in T_h, and stabilizes the H_{II} phase rather than the L_α phase. If we assume that the R_0 value of the DPOPE membrane in water is the same as that of the DOPE membrane in water, we can roughly estimate ΔT_h of the DPOPE membrane owing to the presence of DMSO. Here, we also assume that the decrease in R_0 of the DPOPE membrane induced by DMSO is the same as the decrease in $d/2$. Figure 5 shows that the difference in R_0 of the DPOPE membrane in water and in $X = 0.060$ (DMSO concentration) is 0.4 nm, and Fig. 10 shows that R_0 of the DOPE membrane in water is 2.2 nm. The estimation based on Eq. (8) shows that $\Delta T_h = -8 \times 10$ ($= -80$) K when the DMSO concentration increases from $X = 0$ to 0.060, where we have used the parameters $A_o^{bil} = 62$ Å^2 (Fig. 10), $\Delta S_h = 2.25$ J mol^{-1} K^{-1} for the DPOPE membrane (Epand 1990), and a relatively low value for κ (1×10^{-20} J) (Marsh 1996). From the facts that DMSO induced the L_α to H_{II} phase transition in the DPOPE dispersion at $X_{DMSO} = 0.060$ (Fig. 4) and also that T_h of the DPOPE

membrane in water is 43.2 °C (Epand 1990), the experimentally measured value of ΔT_h was obtained, which shows $\Delta T_h = -23$ K when the DMSO concentration increases from $X = 0$ to 0.060. This value is the same order as that estimated by Eq. (8).

In equilibrium, three kinds of lateral pressure in the membrane have to balance, i.e., $\Pi_{head} + \Pi_{chain} = \Pi_{tot} = \gamma$, where Π_{head} is the repulsive pressure between the headgroups, Π_{chain} is the repulsive chain pressure, Π_{tot} is the total resultant repulsive pressure, and γ is the attractive interfacial pressure due to the hydrophobic interaction between the alkyl chains and water at the membrane surface (Israelachvili 1992). We can assume that γ is almost constant in the presence of various concentrations of DMSO, because DMSO molecules are preferentially excluded from the headgroup region of these membranes under this condition. As discussed in the previous section, the increase in ΔG_i with an increase in DMSO concentration induces the shrinkage of the membrane interface consisting of the surface segments and solvents, which decreases the amount of solvents in the membrane interface, and thereby it reduces the effective cross-sectional area of the phospholipid headgroup regions and also reduces Π_{head}. Therefore, the lateral compression pressure of the membrane, γ–Π_{head}, increases with an increase in DMSO concentration. The results of Fig. 6 show that the fluidity of the DPOPE and the DOPE membranes decreased with an increase in DMSO concentration, suggesting that the lateral compression of the membranes increased. This increase also induces the increase in the chain-melting phase transition temperature, T_m (Fig. 8) of the DEPE membrane. Similar situations, where the increase in the lateral compression pressure induces an increase in T_m, have been observed in other systems (Yamazaki et al. 1992; Kinoshita et al. 1998; Furuike et al. 1999). These results support the above hypothesis.

Rand and his colleagues (Rand et al. 1990; Rand and Fuller 1994) reported the structural dimensions of DOPE membranes in various water concentrations below ϕ_w (weight fraction of water) = 0.3; as the water concentration decreased, the average area of the lipid headgroup at the lipid-water interface decreased, and the average area of the hydrocarbon end of the lipid molecule increased, while the average area at the position near the polar-apolar interface (i.e., polar group-hydrocarbon interface), A_{pp}, remained a constant value. This change in structural dimensions can explain the decrease in R_w (the radius of curvature of the lipid monolayer) with a decrease in water concentration. They defined this position whose area is A_{pp} as the pivotal position (or pivotal plane) because at this position the molecular area stays constant as the monolayer is bent (or curls), and indicated that this area in the H_{II} phase is almost the same as that in the bilayer (L_α) phase. Their results also support our hypothesis that the decrease in solvent content in the membrane interface with an increase in DMSO concentration induces the decrease in R_w of the PE membrane.

Tristram-Nagle et al. (1998) reported that DMSO has a dehydrating effect on the lipid headgroup of DPPC membranes at low concentrations in water. Webb et al. (1993) showed that, in dispersions of DOPE/DOPC, the L_α to H_{II} phase transition occurred at low water content, indicating that the decrease in water content of the head group regions of these membranes may induce the L_α to H_{II} phase transition. These results support our interpretation mentioned above.

On the other hand, in the case of interaction of acetone and the PE membranes, as the acetone concentration in the aqueous phase increases, i.e., the ΔG_{i2} of solvents with hydrophobic alkyl chains decreases, the contact area between the alkyl chains and the solvent increases. This induces an enlargement of the effective cross-sectional area of the phospholipid, which will increase $\Pi_{head,}$ and also decreases γ. Therefore, the lateral compression pressure of the membrane, γ–Π_{head}, decreases and also the packing of the phospholipid alkyl chains decreases with an increase in acetone concentration. The results of Fig. 6 and Fig. 8 support the above speculation. Hence, these effects stabilize the L_α phase more than the H_{II} phase of the PE membranes. The decrease in the packing parameter induces an increase in T_h, and stabilizes the L_α phase rather than the H_{II} phase.

Effect of interaction free energy of the surface segments with solvents on the phase stability of the H_{II} phase and the L_βI phase

We summarize the effect of the interaction free energy of the surface segments with solvents on the phase stability of the H_{II} phase and also another nonbilayer phase, the interdigitated gel (L_βI) phase, in Fig. 12. There is a remarkable resemblance between the phase stability of the H_{II} phase and that of the L_βI phase (Yamazaki 2000). Type A solvents, i.e., water-miscible organic solvents such as acetone, acetonitrile, and ethanol, induce the H_{II} to L_α phase transition in the PE membranes (Kinoshita and Yamazaki 1997) and also the $L_{\beta'}$ to L_βI phase transition in the gel-phase PC membranes (Kinoshita and Yamazaki 1996) above their critical concentrations, and stabilize the L_α phase (relative to the H_{II} phase) and the L_βI phase (relative to the $L_{\beta'}$ phase) (Fig. 12). The type A solvents have a high solubility for alkanes, and hence they induce a decrease in ΔG_{i2}, i.e., the interaction free energy between solvents and the hydrophobic segments of the alkyl chains in the membrane interface. This change of the interaction free energy leads to two important consequences. One is that the contact area of the alkyl chains with solvents increases, inducing an increase in the area of the membrane interface, and as a result the packing parameter of the phospholipid decreases. The other is that the phases having larger contact area of the alkyl chains and solvents, such as the L_α and L_βI phases, are more stabilized than those having a smaller contact area such as the H_{II} and $L_{\beta'}$ phases. This is why, above the critical concentrations of type A

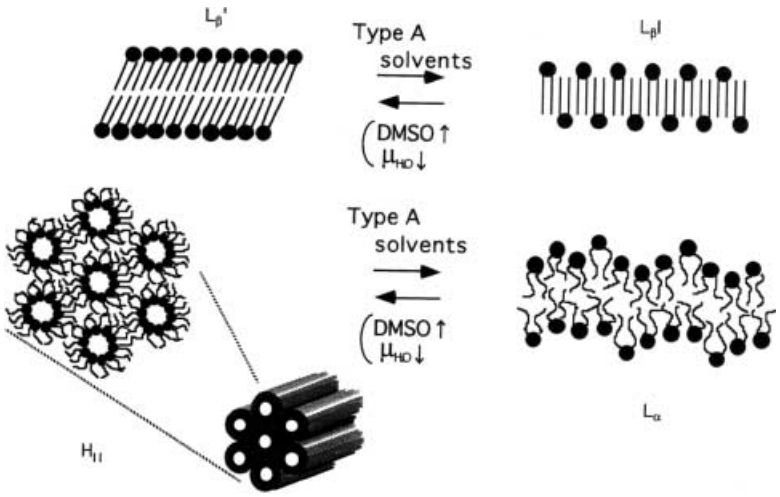

Fig. 12 Effect of various kinds of solvents and the interaction free energy of the surface segments of membranes with solvents on the phase stability of the H_{II} phase and the $L_{\beta}I$ phase. Type A solvents, i.e., water-miscible organic solvents such as acetone, acetonitrile, and ethanol, have a high solubility for alkanes, and hence they induce a decrease in ΔG_{i2}, i.e., the interaction free energy between solvents and the hydrophobic segments of the alkyl chains in the membrane interface. On the other hand, DMSO has a low solubility for alkanes and is also a poor solvent for the hydrophilic segments of the surface of the phospholipid membrane, and thereby induces an increase in ΔG_i, i.e., the interaction free energy between solvents and the surface segments of both the hydrophilic segments and the alkyl chains in the membrane interface

solvents, the L_{α} and the $L_{\beta}I$ phases become more stable, and thereby the H_{II} to L_{α} and the L_{β}' to $L_{\beta}I$ phase transitions occur.

On the other hand, DMSO induces the L_{α} to H_{II} phase transition in the PE membranes (Yu et al. 1996; this paper) and also the $L_{\beta}I$ to L_{β}' phase transition in the gel-phase PC membranes (Yamashita et al. 2000) above their critical concentrations, and stabilizes the H_{II} phase (relative to the L_{α} phase) and the L_{β}' phase (relative to the $L_{\beta}I$ phase) (Fig. 12). DMSO induces an increase in ΔG_i, i.e., the interaction free energy between solvents and the surface segments, of both the hydrophilic segments and the alkyl chains in the membrane interface. This change of ΔG_i leads to two important consequences. One is that the contact area of the segments of membrane surfaces with solvents decreases, inducing a decrease in the area of the membrane interface, and as a result the repulsive interaction between the headgroups of the phospholipids decreases and also the packing parameter of the phospholipid increases. The other is that the phases having a smaller contact area of the surface segments of the membranes and solvents, such as the H_{II} and L_{β}' phases, are more stabilized than those having a larger contact area, such as the L_{α} and $L_{\beta}I$ phases. This is why, above the critical concentrations of DMSO, the H_{II} and L_{β}' phases becomes more stable, and thereby the L_{α} to H_{II} and $L_{\beta}I$ to L_{β}' phase transitions occur.

Based on this analysis of the effect of interaction free energy of the surface segments with solvents on the phase stability of these membranes, we can understand clearly the effect of hydration on the phase stability. To control the hydration of the membrane interface, we usually manipulate the chemical potential of water, μ_{H_2O}, by the osmotic stress method (Rand and Parsegian 1989; Yamazaki et al. 1989, 1992) and by the change of weight fraction of water in solutions. The decrease in μ_{H_2O} induces the L_{α} to H_{II} phase transition in the PE membranes (Seddon and Templer 1995; Fig. 10 in this paper) and also the $L_{\beta}I$ to L_{β}' phase transition in the gel-phase PC membranes (Hatanaka et al. 1997) above its critical values, and stabilizes the H_{II} phase (relative to the L_{α} phase) and the L_{β}' phase (relative to the $L_{\beta}I$ phase) (Fig. 12). This leads to a similar consequence as in the case of DMSO. The decrease in μ_{H_2O} induces a decrease in the area of the membrane interface (Yamazaki et al. 1989, 1992), and as a result the repulsive interaction between the headgroups of the phospholipids decreases and also the packing parameter of the phospholipid increases. Therefore, it induces these phase transitions.

Acknowledgements This work was supported partly by Grant-in Aid for General Scientific Research C (grant 07808073) from the Ministry of Education, Science, and Culture (Japan) to M.Y., by a grant from the Asahi Glass Foundation (Japan) to M.Y, and also by the Satellite Venture Business Laboratory at Shizuoka University to K.K. and M.Y.

References

Ahkong QF, Fischer D, Tampion W, Lucy JA (1975) Mechanism of cell fusion. Nature 253:194–195

Anderson DM, Gruner SM, Leibler S (1988) Geometrical aspects of the frustration in the cubic phases of lyotropic liquid crystals. Proc Natl Acad Sci USA 85:5364–5368

Aota-Nakano Y, Li SJ, Yamazaki M (1999) Effects of electrostatic interaction on the phase stability and structures of cubic phases of monoolein/oleic acid mixture membranes. Biochim Biophys Acta 1461:96–102

Bagatolli LA, Gratton E, Fidelio GD (1998) Water dynamics in glycosphingolipid aggregates studied by Laurdan fluorescence. Biophys J 75:331–341

Bartlett GR (1959) Phosphorus assay in column chromatography. J Biol Chem 234:466–468

Basáñez G, Nieva JL, Rivas E, Alonso A, Goñi FM (1996) Diacylglycerol and the promotion of lamellar-hexagonal and lamellar-isotropic phase transitions in lipids: implications for membrane fusion. Biophys J 70:2299–2306

Bunch W, Edwards C (1969) The permeation of non-electrolytes through the single barnacle muscle cell. J Physiol (London) 202:683–697

Cevc G, Hauser M, Kornyshev AA (1995) Effects of the interfacial structure on the hydration forces between laterally uniform surfaces. Langmuir 11:3103–3110

Chen Z, Rand RP (1997) The influence of cholesterol on phospholipid membrane curvature and bending elasticity. Biophys J 73:267–276

Chen Z, Rand RP (1998) Comparative study of the effects of several n-alkanes on phospholipid hexagonal phases. Biophys J 74:944–952

Chiu S-W, Clark M, Balaji V, Subramaniam S, Scott HL, Jakobsson E (1996) Incorporation of surface tension into molecular dynamics simulation of an interface: a fluid phase lipid bilayer membrane. Biophys J 69:1230–1245

Colotto A, Martin I, Ruysschaert J-M, Sen A, Hui SW, Epand RP (1996) Structural study of the interaction between the SIV fusion peptide and model membranes. Biochemistry 35:980–989

Epand RM (1990) Hydrogen bonding and the thermotropic transitions of phosphatidylethanolamines. Chem Phys Lipids 52:227–230

Furuike S, Levadny VG, Li SJ, Yamazaki M (1999) Low pH induces an interdigitated gel to bilayer gel phase transition in dihexadecylphosphatidylcholine membrane. Biophys J 77:2015–2023

Galla H-J, Hartmann W (1980) Excimer-forming lipids in membrane research. Chem Phys Lipids 27:199–219

Galla H-J, Thelen U, Hartmann W (1979) Transversal mobility in bilayer membrane vesicles: use of pyrene lecithin as optical probe. Chem Phys Lipids 23:239–251

Glatter O, Kratky O (1982) Small angle X-ray scattering. Academic Press, New York

Gordeliy VI, Kiselev MA, Lesieur P, Pole AV, Teixeira J (1998) Lipid membrane structure and interactions in dimethyl sulfoxide/water mixtures. Biophys J 75:2343–2351

Gruner SM (1985) Intrinsic curvature hypothesis for biomembrane lipid composition: a role for nonbilayer lipids. Proc Natl Acad Sci USA 82:3665–3669

Gruner SM, Cullis PR, Hope MJ, Tilcock CPS (1985) Lipid polymorphism: the molecular basis of nonbilayer phases. Annu Rev Biophys Biophys Chem 14:211–238

Gruner SM, Tate MW, Kirk GL, So PTC, Turner DC, Keane DT, Tilcock CPS, Cullis PR (1988) X-ray diffraction study of the polymorphic behavior of N-methylated dioleoylphosphatidylethanolamine. Biochemistry 27:2853–2866

Hatanaka Y, Kinoshita K, Yamazaki M (1997) Osmotic stress induces a phase transition from interdigitated gel phase to bilayer gel phase in multilamellar vesicles of dihexadecylphosphatidylcholine. Biophys Chem 65:229–233

Hayakawa E, Naganuma M, Mukasa K, Shimozawa T, Araiso T (1998) Change of motion and localization of cholesterol molecule during L_{α}-H_{II} transition. Biophys J 74:892–898

Helfrich W (1978) Steric interaction of fluid membranes in multilayer systems. Z Naturforsch A 33:305–315

Hui S-W, Sen A (1989) Effects of lipid packing on polymorphic phase behavior and membrane properties. Proc Natl Acad Sci USA 86:5825–5829

Israelachvili JN (1992) Intermolecular and surface forces, 2nd edn. Academic Press, New York

Israelachvili JN, Wennerström H (1996) Role of hydration and water structure in biological and colloidal interactions. Nature 379:219–225

Kinoshita K, Yamazaki M (1996) Organic solvents induce interdigitated gel structures in multilamellar vesicles of dipalmitoylphosphatidylcholine. Biochim Biophys Acta 1284: 233–239

Kinoshita K, Yamazaki M (1997) Phase transition between hexagonal II (H_{II}) and liquid-crystalline phase induced by interaction between solvents and segments of the membrane surface of dioleoylphosphatidylethanolamine. Biochim Biophys Acta 1330:199–206

Kinoshita K, Asano T, Yamazaki M (1997) Interaction of the surface of biomembrane with solvents: structure of multilamellar vesicles of dipalmitoylphosphatidylcholine in acetone-water mixtures. Chem Phys Lipids 85:53–65

Kinoshita K, Furuike S, Yamazaki M (1998) Intermembrane distance in multilamellar vesicles of phosphatidylcholine depends on the interaction free energy between solvents and the hydrophilic segments of the membrane surface. Biophys Chem 74:237–249

Kirk GL, Gruner SM (1985) Lyotropic effects of alkanes and headgroup composition on the L_{α}-H_{II} lipid liquid crystal phase transition: hydrocarbon packing versus intrinsic curvature. J Phys (Paris) 46:761–769

Kirk GL, Gruner SM, Stein DL (1984) A thermodynamic model of the lamellar to inverse hexagonal phase transition of lipid membrane-water system. Biochemistry 23:1093–1102

Kozlov MM, Leikin S, Rand RP (1994) Bending, hydration and interstitial energies quantitatively account for the hexagonal-lamellar-hexagonal reentrant phase transition in dioleoylphosphatidylethanolamine. Biophys J 67:1603–1611

Kruijff B de (1997). Lipids beyond the bilayer. Nature 386:129–130

Lipowsky R (1991) The conformation of membranes. Nature 349:475–481

Luzzati V (1997) Biological significance of lipid polymorphism: the cubic phases. Curr Opin Struct Biol 7:661–668

Luzzati V, Husson F (1962) X-ray diffraction studies of lipid-water systems. J Cell Biol 12:207–219

Marsh D (1996) Intrinsic curvature in normal and inverted lipid structures and in membranes. Biophys J 70:2248–2255

Nagel JF, Wilkinson DA (1978) Lecithin bilayers. Density measurement and molecular interactions. Biophys J 23:159–175

Nagle JF, Zhang R, Nagle S-T, Sun W, Petrache HI, Suter RM (1996) X-ray structure determination of fully hydrated Lα phase dipalmitoylphosphatidylcholine bilayers. Biophys J 70:1419–1431

Parasassi T, Stasio GD, Ravagnan G, Rusch RM, Gratton E (1991) Quantitation of lipid phases in phospholipid vesicles by the generalized polarization of Laurdan fluorescence. Biophys J 60:179–189

Pebay-Peyroula E, Rummel G, Rosenbusch JP, Landau EM (1997) X-ray structure of bacteriorhodopsin at 2.5 angstroms from microcrystals grown in lipidic cubic phases. Science 277:1676–1681

Perkins WR, Dause RB, Parente RA, Minchey SR, Neuman KC, Gruner SM, Taraschi TF, Janoff AS (1996) Role of lipid polymorphism in pulmonary surfactant. Science 273:330–332

Rand RP, Fuller NL (1994) Structural dimensions and their changes in reentrant hexagonal-lamellar transition of phospholipids. Biophys J 66:2127–2138

Rand RP, Parsegian VA (1989) Hydration forces between phospholipid bilayers. Biochim Biophys Acta 988:351–376

Rand RP, Fuller NL, Gruner SM, Parsegian VA (1990) Membrane curvature, lipid segregation, and structural transition for phospholipids under dual-sovent stress. Biochemistry 29:76–87

Sackmann E (1996) Supported membranes: scientific and practical applications. Science 271:43–48

Sassaroli M, Vauhkonen M, Perry D, Eisinger J (1990) Lateral diffusivity of lipid analogue excimeric probes in dimyristoylphosphatidylcholine bilayers. Biophys J 57:281–290

Seddon JM, Templer RH (1995) Polymorphism of lipid-water systems. In: Lipowsky R, Sackmann E (eds) Structure and dynamics of membranes. Elsevier, Amsterdam, pp 97–160

Smondyrev AM, Berkowitz ML (1999) Molecular dynamics simulation of DPPC bilayer in DMSO. Biophys J 76:2472–2478

Tate MW, Gruner SM (1989) Temperature dependence of the structural dimensions of the inverted hexagonal (HII) phase of phosphatidylethanolamine-containing membranes. Biochemistry 28:4245–4253

Tristram-Nagle S, Moore T, Petrache HI, Nagle JF (1998) DMSO produces a new subgel phase in DPPC: DSC and X-ray diffraction study. Biochim Biophys Acta 1369:19–33

Tu K, Tobias DJ, Blasie K, Klein ML (1996) Molecular dynamics investigation of the structure of a fully hydrated gel-phase dipalmitoylphosphatidylcholine bilayers. Biophys J 70:595–608

Ulrich AS, Watts A (1994) Molecular response of the lipid headgroup to bilayer hydration monitored by ^{2}H-NMR. Biophys J 66:1441–1449

Vaismann II, Berkowitz ML (1992) Local structural order and molecular associations in water-DMSO mixtures. Molecular dynamics study. J Am Chem Soc 114:7889–7896

Webb MS, Hui SW, Steponkus PL (1993) Dehydration-induced lamellar-to-hexagonal-II phase transitions in DOPE/DOPC mixtures. Biochim Biophys Acta 1145:93–104

Wiener MC, White SH (1992) Structure of a fluid dioleoylphosphatidylcholine bilayer determined by joint refinement of X-ray and neutron diffraction data. III. Complete structure. Biophys J 61:434–447

Yamashita Y, Kinoshita K, Yamazaki M (2000) Low concentration of DMSO stabilizes the bilayer gel phase rather than the interdigitated gel phase in dihexadecylphosphatidylcholine membrane. Biochim Biophys Acta 1467:395–405

Yamazaki M (2000) Solvation of biomembranes. In: Nagayama K (ed) Water and life – from thermodynamics to physiology. (Series new biophysics II-2) Kyoritsu, Tokyo, pp 79–96

Yamazaki M, Ohnishi S, Ito T (1989) Osmoelastic coupling in biological structures: decrease in membrane fluidity and osmophobic association of phospholipid vesicles in response to osmotic stress. Biochemistry 28:3710–3715

Yamazaki M, Ohshika M, Kashiwagi N, Asano T (1992) Phase transition of phospholipid vesicles under osmotic stress and in the presence of ethylene glycol. Biophys Chem 43: 29–37

Yu Z-W, Quinn PJ (1995) Phase stability of phosphatidylcholines in dimethyl sulfoxide solutions. Biophys J 69:1456–1463

Yu Z-W, Williams WP, Quinn PJ (1996) Thermotropic properties of dioleoylphosphatidylethanolamine in aqueous dimethyl sulfoxide solutions. Arch Biochem Biophys 332:187–195